A Note on the Relationship of Temperature and Water Vapor over Oceans, as well as the Sea Surface Temperature Impact

by

C.-L. Shie[1,2], W.-K. Tao[2] and J. Simpson[2]

[1]Goddard Earth Sciences and Technology Center
University of Maryland, Baltimore County
Baltimore, Maryland 21250

[2]Laboratory for Atmospheres
NASA Goddard Space Flight Center
Greenbelt, Maryland 20771

A Special Issue of Advances in Atmospheric Sciences

(February 15, 2005)

Corresponding author address: Dr. Chung-Lin Shie, Mesoscale Atmospheric Processes Branch, Code 613.1, NASA/GSFC, Greenbelt, MD 20771

E-mail: shie@agnes.gsfc.nasa.gov

Phone number: 301-614-6312

Fax number: 301-614-5492

Abstract

This note follows up on a recent study by Shie et al. (2005) and extends the investigation of the domain-averaged moisture-temperature (Q-T) relationship from the Tropics (i.e., the previous study) to the three tropical oceans (i.e., the Pacific, Atlantic and Indian Oceans) using the GEOS-3 [Goddard EOS (Earth Observing System) Version-3] global re-analysis monthly products. Similar to the Tropics, a positively correlated Q-T distribution is found over the entire oceanic region. This oceanic regime falls within the lower bound of the tropical regime embedded in a global, curvilinear Q-T relationship. Q, however, increases faster with T over oceans than over the Tropics. A positive correlation is also found between T and SST (sea surface temperature), which suggests that more heat may be needed over open oceans during the colder season to increase the temperature of an air mass by the same amount as compared to the warm season. Q and SST are also found to be positively correlated in a manner that quantitatively resembles an earlier result found by Stevens (1990). Relative humidity (RH) exhibits similar behaviors for oceanic and tropical regions, respectively. RH increases with increasing SST and T over oceans and increases with increasing T in the Tropics (Shie et al. 2005). The similar features found between oceanic and tropical regions seem to imply that oceans occupy most of the Tropics and so play a key role in determining the tropical climate.

T, Q, saturated water vapor, RH, and SST are also examined with regard to the warm and cold "seasons" over individual oceans. The Indian Ocean warm season dominates in each of the five quantities, while the Atlantic Ocean cold season has the lowest values in most categories. The higher values for the Indian Ocean may be due to its relatively high percentage of tropical coverage compared to the other two oceans. However, Q is found to increase faster for colder months from individual oceans, which differs from the general finding in the global Q-T relationship that Q increases slower for colder climate. The modified relations might be

attributed to the small sample size used in each individual oceanic group, or are possibly an oceanic impact.

1. Introduction

In a very recent study (Shie et al. 2005), an ideal and simple formulation was derived that well represented a quasi-linear relationship found between the domain-averaged water vapor, q (mm), and temperature, T (K), fields for the Tropics based on the numerical data obtained from a series of quasi-equilibrium (long-term) simulations using a two-dimensional Goddard Cumulus Ensemble (GCE) model (Tao et al. 1999, Tao et al. 2001, and Shie et al. 2003) and the GEOS-3 [Goddard EOS (Earth Observing System) Version-3] global re-analysis monthly products (Hou et al. 2001), along with a handful of observations[1]. In Shie et al. 2005, the water vapor-temperature relationship for the extra-tropical regions, i.e., mid- and high latitudes was, however, found more complex by using the readily available GEOS-3 global re-analysis monthly products. The tropical quasi-linear temperature-moisture relation was found embedded in a globally curvilinear moisture-temperature distribution that was similar to the famous Clausius-Clapeyron curve, i.e., the saturated water vapor pressure increases faster/slower at a higher/lower temperature. In the earlier studies (Tao et al. 1999 and Shie et al. 2003), the forced maintenance of two different wind profiles was found dynamically critical to determine the various tropical quasi-equilibrium states. The similarity between a curvilinear global moisture-temperature distribution (in macro-scale) and an exponentially varying saturated water vapor pressure-temperature relationship (in micro-scale) seemed to clarify that the dynamics were crucial to determine a climate (or a quasi-equilibrium state) but the thermodynamics adjusted the magnitude. The corresponding relative humidity and temperature fields, however, showed a two-branch relationship (Shie et al. 2005). In the Tropics, relative humidity increased more rapidly with increasing temperature due to a faster increase of moisture than saturated moisture,

[1] Observations examined includes the Marshall Islands sounding (used for the GCE simulations), two of the major TRMM (Tropical Rainfall Measuring Mission -- Simpson et al. 1996) field experiments [i.e., SCSMEX (the 1998 South China Sea Monsoon Experiment -- Lau et al. 2000) and KWAJEX (the 1999 Kwajalein Atoll field experiment -- Yuter et al. 2004)] as well as from two other field experiments [i.e., TOGA-COARE (Tropical Ocean and Global Atmosphere Coupled Ocean-Atmosphere Response Experiment

while in mid- and high latitudes, relative humidity roughly decreased with increasing temperature due to a slower increase of moisture than saturated moisture.

Stephens (1990) found a positive correlation between monthly mean precipitable water and sea surface temperature by using 52 months of precipitable water from passive microwave radio and NMC (National Meteorological Center global) gridded SST dataset blended with in situ and satellite observations. It also showed that such analyses based on global or regional scale resulted in differences in both phase and amplitude that could be used as a tracer of large-scale circulation. The purpose of this study (i.e., a continuation of Shie et al. 2005) is, therefore, to extend an investigation on the water and energy cycle into three major tropical oceans, i.e., Pacific, Atlantic and Indian Oceans for relatively 'warm/moist" and "cold/dry" regimes. Basic goals of this note are simply to clarify (1) whether the water vapor-temperature or relative humidity-temperature relations for the respective oceanic regions would resemble or differ from those found in the Tropics? (2) What the impact sea surface temperature (SST) may have on those relations? The correlated SST signature and large-scale circulation suggested in Stephens (1990) is a feature that will not be examined in this study.

The GEOS-3 re-analysis data used in this note are described in section 2. The aforementioned idealized theoretical formulation that represents slopes of the domain-averaged water vapor and temperature distributions (Shie et al. 2005) is adopted and brief discussed in section 3. Section 4 presents the major findings for the oceanic regions, as well as comparisons with earlier findings in Shie et al. 2005. A final remark is given in section 5.

2. Data

-- Webster and Lukas 1992) and GATE (Global Atmospheric Research Programme Atlantic Experiment -- Houze and Betts 1981)].

The eleven monthly GEOS-3 global re-analysis data used in Shie et al. 2005 for studying the global and tropical water vapor-temperature relationship are continually used in this study to obtain the temperature, water vapor, and SST fields for the three targeted oceanic regions, i.e., Pacific, Atlantic, and Indian Oceans. These monthly-averaged GEOS-3 re-analysis data include (1) seven "summer" months – May, June, July and August in 1998 for SCSMEX and July, August and September in 1999 for KWAJEX, and (2) four "winter" months – January, February, November, and December in 1998. The GEOS-3 "summer" months were intended to match the SCSMEX and KWAJEX periods, while the "winter" months were chosen for the same year as SCSMEX - 1998. The GEOS-3 seven "summer" and four "winter" months are sorted into three oceanic regions approximating "Pacific" (22^0S-22^0N, 120^0E-120^0W), "Atlantic" (22^0S-22^0N, 65^0W-15^0W), and "Indian" (22^0S-10^0N, 40^0E-110^0E) Oceans, respectively.

3. Idealized Formulation

According to Shie et al. 2005, for an equilibrium state, the domain (i.e., horizontally and vertically) averaged or integrated equations for potential temperature (θ) and water vapor (mixing ratio, q_v) can be reduced to

$$C_p \frac{\partial[\overline{T}]}{\partial t} = 0, \tag{1}$$

and

$$L_v \frac{\partial\{\overline{q}_v\}}{\partial t} = 0 \tag{2}$$

where $[\overline{T}]$ and $\{\overline{q_v}\}$ are the domain-averaged and density-weighted temperature (K), and the vertically integrated column water vapor (mm) (so called "precipitable water"), respectively, as overbar represents horizontal-averaged quantities. The units for $\{\overline{q_v}\}$ are in mm since $\overline{q_v}$ ($g\ kg^{-1}$) has been integrated along a vertical column with the vertical scale height becoming implicit. Curly parentheses are thus used to denote such a vertical integral for water vapor to distinguish from the brackets that represent a vertical average for temperature (along with an explicit vertical scale height). C_p and L_v are the specific heat of dry air at constant pressure and the latent heats of condensation, respectively.

The vertically integrated static energy densities ($J\,m^{-2}$) from the domain-averaged temperature and water vapor, respectively, at an occurred equilibrium state, which depend on τ that represents various equilibrium states, can then be represented as follows:

$$C_1(\tau) = C_p \tilde{\overline{\rho}}_{air} [\overline{T}] H, \tag{3}$$

$$C_2(\tau) = L_v \tilde{\overline{\rho}}_w \{\overline{q_v}\} \tag{4}$$

where $\tilde{\overline{\rho}}_{air}$ and $\tilde{\overline{\rho}}_w$ are the domain-averaged air and water vapor densities, H the vertical scale height of the free atmosphere. By taking the derivative of equation (4) over equation (3) and assuming that $\tilde{\overline{\rho}}_{air}$ and $\tilde{\overline{\rho}}_w$ are invariant with various quasi-equilibrium state, and the derivative change of L_v with temperature is negligible, a theoretical relationship between the variations of water vapor and temperature with respect to quasi-equilibrium state can then be obtained as follows

$$\frac{d\{\overline{q_v}\}}{d[\overline{T}]} = (C_p \bar{\bar{\rho}}_{air} H / L_v \bar{\bar{\rho}}_w) \frac{dC_2}{dC_1}(\tau). \tag{5}$$

By assuming that $\bar{\bar{\rho}}_w$ and $\bar{\bar{\rho}}_{air}$ are 10^3 and 1 $kg\ m^{-3}$, respectively, and H is 10 km, equation (5) can be further simplified as

$$\frac{d\{\overline{q_v}\}}{d[\overline{T}]} = C_{ideal} \frac{dC_2}{dC_1}(\tau) \tag{6}$$

where $C_{ideal} = (C_p / L_v)(10^4\, mm)$ that increases from 4.016 ($mm\ K^{-1}$) to 4.462 ($mm\ K^{-1}$) as L_v decreases from 2.5×10^6 J kg^{-1} (at 0^0C) to 2.25×10^6 J kg^{-1} (at 100^0C) at a C_p of 1004 J $(K\ kg)^{-1}$. Equation (6) provides a simplified theoretical relationship for the derivative of $\{\overline{q_v}\}$ and $[\overline{T}]$ that depends on a near constant C_{ideal} [e.g., 4.239 ($mm\ K^{-1}$), a mean of 4.016 ($mm\ K^{-1}$) and 4.462 ($mm\ K^{-1}$)] and a various dC_2/dC_1. Generally speaking, the moisture-temperature slope is proportional to the derivative of static energy contributions (dC_2/dC_1) by a factor of C_{ideal}.

4. Results

The domain-averaged water vapor versus temperature obtained from eleven months of GEOS-3 data for three oceanic regions - "Atlantic" (22^0S-22^0N, 65^0W-15^0W), "Indian" (22^0S-10^0N, 40^0E-110^0E) and "Pacific" Oceans (22^0S-22^0N, 120^0E-120^0W), respectively, are shown in Fig. 1. Each oceanic group is divided into "warm" and "cold" regimes based on a criterion air temperature of 258.5 K that is near an averaged temperature including all the oceanic data examined (see details in Table 1 shown later). A linear regression method built into the plotting package ("KaleidaGraph") that produced the scatter plot has also been applied

to the entire data group shown in Fig. 1 to obtain a regression line. The moist and temperature relationship based on the entire oceanic data (Fig. 1) will be discussed first, and then features involving individual oceans will be brief presented later (in the end of this section) mainly based on Table 1. A positive water vapor–temperature correlation (i.e., a dC_2/dC_1 value of 1.60) obtained based on the regression line consisting of data from all three oceanic groups (Fig. 1) is slightly larger than that found in the Tropics (i.e., a dC_2/dC_1 value of 1.318 in Shie et al. 2005). It implies that the overall oceanic regions favor a quicker increasing in water vapor with increasing temperature than the Tropics does. The domain-averaged moist-temperature data obtained from the global regions (i.e., 135 data points collected from Tropics and mid-, high-latitudes shown in Fig. 4 of Shie et al. 2005) are also included here and drawn together with the oceanic moist-temperature data (shown in Fig. 1) in Fig. 2. Fig. 2 shows that the oceanic moist-temperature data (i.e., 27-55 mm/257-260.5 K denoted as open squares) reside within the lower bound of the tropical moist/temperature range (i.e., 30-86 mm/255-265 K based on [Shie et al. 2005]). The oceanic data show a steeper slope relative to the tropical regions (as mentioned earlier) that are embedded in the global data (crosses) with a curvilinear distribution (the curve on the left hand side). Such a curvilinear distribution bears a remarkable resemblance to the famous Clausius-Clapeyron curve of saturated water vapor pressure (mb)-temperature (dark diamonds and the thick dashed line on the right hand in Fig.2). Detailed discussions can be found in Shie et al. 2005. Note that the dC_2/dC_1 values for the six individual "seasonal" oceanic groups (the corresponding regression lines are not shown in Fig. 1), however, distinguish between "warm and cold seasons", i.e., warm months have smaller values (0.98, 1.32, and 1.76), while cold months tend to own larger values (i.e., 2.16, 2.35 and 3.23). It implies that water vapor increases faster/slower for colder/warmer climate, which apparently differs from what has been generally found in the curvilinear moisture-temperature relationship (Fig. 2) that water vapor increases slower/faster for colder/warmer climate. It is suspected that such modified relations may be primarily attributed to a small sample size in each individual

oceanic group (i.e., seven and four months for summer and winter, respectively), or a possible genuine impact by oceans. It demands an extensive study using a larger data population to confirm one way or the other.

As mentioned in introduction, a positive correlation was found between monthly mean precipitable water and sea surface temperature based on 52 months of precipitable water from passive microwave radio and NMC blended SST (Stevens 1990). Similar feature is also found in this note, yet with less data samples (i.e., 11 months used here versus 52 months). The corresponding domain-averaged SST versus temperature obtained from GEOS-3 for the six "seasonal" ocean groups are shown in Fig. 3 with the open and dark circles denoting data from the "warm" and "cold" months, respectively. Similar to the positively correlated moisture and temperature shown in Fig. 1, SST also generally increases with increasing temperature (T). Based on the slope value obtained for the regression line (thick dashed line in Fig. 3), there is about 1.2 degrees of SST change for one degree of temperature change; however, SST changes slightly less (i.e., 1.1 degrees) for the warm months than for the cold months (i.e., 1.25 degrees) based on the corresponding slopes that are not shown in Fig. 3. It seemingly indicates that more/less heat is needed for an open ocean to maintain an air mass above it (the ocean) with a same degree of temperature increase during a colder/warmer season (or in a colder/warmer region). Again, more data samples will be necessary in a future study to further confirm such an argument.

The domain-averaged water vapor and saturated water vapor (mm) for the six "seasonal" ocean groups are shown versus SST (K) in Fig. 4 with the dark and open circles/triangles denoting water vapor/saturated water vapor from the warm and cold months, respectively. The respective regression lines are obtained including all the water vapor (thick dashed line) and saturated water vapor (thick dotted line) data points. Based on the two respective curves shown in Fig. 4, both water vapor and water vapor pressure increase as SST increase, yet the former

has a faster increase than the latter, particularly for a higher SST. As such, the corresponding relative humidity fields (i.e., the thick solid regression curve) are found increasing with SST. Note that the individual relative humidity data points are not shown in Fig. 4 for the sake of figure clarity. The positively correlated water vapor (or precipitable water) and SST shown in Fig. 4 (thick dashed line) quantitatively agree well with the results found in Stephens (1990). Accordingly, water vapor increasing from 32 mm (equivalent to 3.2 g cm^{-1}) at 298.5 K (around 25.3 C) to 54 mm (5.4 g cm^{-1}) at 303 K (around 29.8 C) shown in Fig. 4 resembles an increasing of precipitable water from 3.4 g cm^{-1} at 25 C to 5.2 g cm^{-1} at 30 C shown in Fig. 6 of Stephens (1990). Similar patterns shown in Fig. 4 can also be attained by replacing SST with temperature (not shown). For example, one of the major features found in the tropical regions (Shie et al. 2005) showing water vapor varying faster/slower for a warmer/colder temperature is also repeated here by replacing SST with T. In Shie et al. 2005, relative humidity fields were also found increasing with increasing temperature in the Tropics due to a faster increase of moisture than saturated moisture as temperature increases. Apparently, the three oceans that occupy most of the Tropics must have played a crucial role in determining the tropical hydrological cycles. However, relative humidity decreased with increasing temperature for mid- and high latitudes (see details in Shie et al. 2005). The different moisture-temperature relations between the Tropics and the extra-tropical regions remain as an interesting topic for future studies.

Discussions presented so far in this section mainly focus on general features involving the three oceans data altogether. The respective domain averaged temperature T, water vapor Q, saturated water vapor Qs, relative humidity RH, and sea surface temperature SST from the warm and cold months for Pacific, Atlantic, and Indian Oceans are listed in Table 1, along with the averaged values for each of the three oceans (listed within parentheses), and a total average from the three oceans altogether (listed in the bottom row). As for each of the individual "seasonal" groups, warm Indian leads with the highest temperature of 259.3 K followed by warm Pacific

(259.1 K), warm Atlantic (258.9 K), cold Indian and Pacific (both 258.1 K), and cold Atlantic (257.7 K). The corresponding Q, Qs, RH and SST also generally follow the same order as T except that cold Atlantic has a slightly larger RH (42.7 %) than cold Pacific (41.4%). Indian Ocean has a locally highest temperature for both warm and cold months that might be due to its relatively high percentage of tropical coverage compared to the two other counterpart oceans. However, the aforementioned features involving each individual ocean may not be considered as conclusive until more monthly data will be included and analyzed in the future study. As for the average quantities for each individual ocean, Indian and Pacific Ocean alternate the leading role among the three oceans as the former dominates in Q, RH and SST, and the latter leads in T and Qs with Atlantic Ocean trailing in a distant third place in each of the five categories. Atlantic Ocean may be fairly considered as the coldest (for both SST and T)/driest ocean among the three in this study.

5. Concluding Remarks

By applying eleven months of GEOS-3 data to three oceanic regions - Atlantic, Indian and Pacific Oceans, an overall positively correlated moisture-temperature distribution is found located near the lower bound of the tropical regime embedded in a globally curvilinear moisture-temperature relationship (Fig. 2). The overall oceanic regime, however, has a steeper slope (i.e., a larger dC_2/dC_1 value) than the Tropics that implies a quicker increasing in water vapor with increasing temperature over oceans. As expected, the air temperature over oceans is found increasing with increasing SST. This positive T-SST correlation further suggests that more/less heat may be needed for an open ocean during a colder/warmer season (or in a colder/warmer region) to maintain an air mass with a same degree of temperature increase. A positive correlation between moisture and SST is also found in this note, which quantitatively resembles the results found in Stevens (1990) even though the sample size used in this study is about one order smaller than that in Stevens (1990). Relative humidity is another quantity that bears

similar features in the oceanic and tropical regions, respectively. Accordingly, RH increases with increasing SST, as well as temperature over oceans, as it also increases with increasing temperature in the Tropics (Shie et al. 2005). The three targeted oceans occupying most of the Tropics must have played a key role in determining the tropical climate. Relative humidity was, however, found decreasing with increasing temperature for mid- and high latitudes (Shie et al. 2005). What major mechanisms might have caused such different moisture-temperature relations between the Tropics and the extra-tropical regions remains an interesting topic for future studies.

The domain-averaged temperature, water vapor, saturated water vapor, relative humidity, and sea surface temperature are also brief examined for the respective "seasons" (i.e., warm and cold months) and oceans (i.e., Pacific, Atlantic, and Indian Oceans). "Warm" Indian is found leading in each of the five studied quantities, while "cold" Atlantic trails in most categories. The dominance by Indian Ocean may be due to its relatively high percentage of tropical coverage compared to the other two counterpart oceans. As the moisture-temperature distributions are examined with respective warm and cold months, it is found that water vapor increases faster/slower for colder/warmer climate, which differs from the general finding shown in the curvilinear moisture-temperature relationship (Fig. 2) that water vapor increases slower/faster for colder/warmer climate. Such modified relations may be primarily attributed to a small sample size used in each individual oceanic group, or a possible oceanic impact. Nonetheless, the aforementioned features involving the individual ocean may not be considered as conclusive until an extensive data population will be included and analyzed in the future.

6. Acknowledgments

The authors wish to thank Dr. A. Hou and Ms. S. Zhang for kindly providing us their GEOS-3 global reanalysis temperature, water vapor, and sea surface temperature fields. This

study is supported by the NASA Headquarters Physical Climate Program and by the NASA TRMM project. The authors are also grateful to Dr. R. Kakar (NASA/HQ) for his support of this research. Acknowledgment is also made to NASA/Goddard Space Flight Center for computer time used in the research.

7. References

Grabowski, W. W., M. W. Moncrieff, and J. T. Kiehl, 1996: Long-term behavior of precipitating tropical cloud systems: A numerical study. *Quart. J. Roy. Meteor. Soc.*, **122**, 1019-1042.

Held, I. M., R. S. Hemler, and V. Ramaswamy, 1993: Radiative-convective equilibrium with explicit two-dimensional moist convection. *J. Atmos. Sci.*, **50**, 3909-3927.

Hou, A. Y., S. Zhang, A. da Silva, W. Olson, C. Kummerow, and J. Simpson, 2001: Improving global analysis and short-range forecast using rainfall and moisture observations derived from TRMM and SSM/I passive microwave sensors. *Bull. Amer. Meteor. Soc.*, **81**, 659-679.

Islam, S., R. L. Bras, and K. A. Emanuel, 1993: Predictability of mesoscale rainfall in the Tropics. *J. Appl. Meteor.*, **32**, 297-310.

Lau, K. M., Y. Ding, J.-T. Wang, R. Johnson, T. Keenan, R. Cifelli, J. Geriach, O. Thiele, T. Rickenbach, S.-C. Tsay, and P.-H. Lin, 2000: A report of the field operations and early results of the South China Sea Monsoon experiment (SCSMEX). *Bull. Amer. Meteor. Soc.*, **81**, 1261-1270.

Randall, D. A., Q. Hu, K.-M. Xu, and S. K. Krueger, 1994: Radiative-convective disequilibrium. *Atmos. Res.*, **31**, 315-327.

Robe, F. R., and K. A. Emanuel, 1996: Dependence of tropical convection on radiative forcing. *J. Atmos. Sci.*, **53**, 3265-3275.

Shie, C.-L. , W.-K. Tao, J. Simpson and C.-H. Sui, 2003: Quasi-equilibrium states in the tropics simulated by a cloud-resolving model. Part 1: Specific features and budget analyses. *J. Climate*, 16, 817-833.

Shie, C.-L. , W.-K. Tao, J. Simpson and C.-H. Sui, 2005: A note on the relationship between temperature and water vapor in quasi-equilibrium and climate states. *J. Climate* (submitted)

Simpson, J., C. Kummerow, W.-K. Tao and R. Adler, 1996: On the Tropical Rainfall Measuring Mission (TRMM). *Meteor. and Atmos. Phys.*, 60, 19-36.

Stephens, G. L., 1990: On the relationship between water vapor over the oceans and sea surface temperature. *J. Climate*, 3, 634-645.

Sui, C.-H., K. M. Lau, W.-K. Tao, and J. Simpson, 1994: The tropical water and energy cycles in a cumulus ensemble model. Part I: Equilibrium climate. *J. Atmos. Sci.*, **51**, 711-728.

Tao, W.-K., and J. Simpson, 1993: The Goddard Cumulus Ensemble Model. Part I: Model description. *Terr. Atmos. Oceanic Sci.*, **4**, 35-72.

____, C.-H. Sui, C.-L. Shie, B. Zhou, K. M. Lau, and M. Moncrieff, 1999: On equilibrium (climate) states simulated by cloud-resolving models. *J. Atmos. Sci.*, **56**, 3128-3139.

____, C.-L. Shie, and J. Simpson, 2001: Comments on "A sensitivity study of radiative-convective equilibrium in the tropics with a convection-resolving model". *J. Atmos. Sci.*, **58,** 1328-1333.

Webster, P. J., and R. Lukas, 1992: TOGA COARE: The Coupled Ocean-Atmosphere Response Experiment. *Bull. Amer. Meteor. Soc.*, **73**, 1377-1416.

Wu, X. and M. W. Moncrieff, 1999: Effects of sea surface temperature and large-scale dynamics on the thermodynamic equilibrium state and convection over the tropical western Pacific. *J. Geophys. Res.*, **104**, 6093-6100.

Xu, K.-M., and D. A. Randall, 1999: A sensitivity study of radiative-convective equilibrium in the tropics with a convection-resolving model. *J. Atmos. Sci.*, **56**, 3385-3399.

Yuter, S., R. A. Houze Jr., E. A. Smith, T. T. Wilheit, E. Zipser, 2003: Physical characterization of tropical oceanic convection observed in KWAJEX. *J. Appl. Meteor.*. (submitted)

Table 1. The domain averaged temperature T (K), water vapor Q (mm), saturated water vapor Qs (mm), relative humidity RH (%), and sea surface temperature SST (K) for the warm, cold, and entire region of Pacific, Atlantic, Indian Ocean, respectively. The relatively warm and cold regimes are divided based on a criterion temperature of 258.5 (K) that is chosen near the averaged temperature from all the oceanic data, i.e., 258.6 (K).

	T (K)		Qs (mm)		
	259.1/258.1 (258.9)		69.0/62.8 (67.6)		
	258.9/257.7 (258.2)		68.6/61.8 (64.9)		
	259.3/258.1 (258.8)		71.1/62.9 (67.4)		
	258.6		66.6		

Figure captions:

Fig. 1. Scatter diagram of domain-averaged water vapor versus temperature for three oceanic regions - "Atlantic" (22^0S-22^0N, 65^0W-15^0W), "Indian" (22^0S-10^0N, 40^0E-110^0E) and "Pacific" Ocean (22^0S-22^0N, 120^0E-120^0W), respectively, in "warm" (denoted as "wm") and "cold"(denoted as "cd") months. The relatively warm and cold regimes are divided based on a criterion temperature of 258.5 (K) (see details in Table 1). A regression line (thick dotted line) with a slope of 6.8 (mm K^{-1}) obtained by applying a linear regression method to the group including all data points is also shown.

Fig. 2. The oceanic domain-averaged water vapor (mm)-temperature (K) (also shown in Fig. 1) (open squares), along with the curvilinear distribution of domain-averaged water vapor-temperature for 135 data points from global regions (crosses and solid curve) and the curvilinear distribution of saturated water vapor pressure (mb)-temperature obtained based on the Clausius-Clapeyron equation (dark diamonds and dashed curve) (adopted from Fig. 4 in Shie et al. 2005). The curvilinear lines are obtained using an exponential fitting.

Fig. 3. Scatter diagram of domain-averaged SST versus temperature for the six "seasonal" ocean groups (same as those in Fig. 1) with the open and dark circles denoting data from the "Cold" and "Warm" months, respectively. A regression line (thick dashed line) with a slope of 1.2 (K K^{-1}) obtained by applying a linear regression method to the group including all data points is also shown.

Fig. 4. The distribution of domain-averaged water vapor and saturated water vapor (mm) versus SST (K) for the six "seasonal" ocean groups (same as those in Fig. 1) with the dark

and open circles/triangles denoting water vapor/saturated water vapor from the warm and cold months, respectively. The respective curvilinear lines are obtained including all the water vapor (thick dashed line) and saturated water vapor (thick dotted line) data points using an exponential regression fitting. A regression line obtained by including all the relative humidity (%) data points is also shown (thick solid line). The individual relative humidity data points are not shown here for the sake of figure clarity.

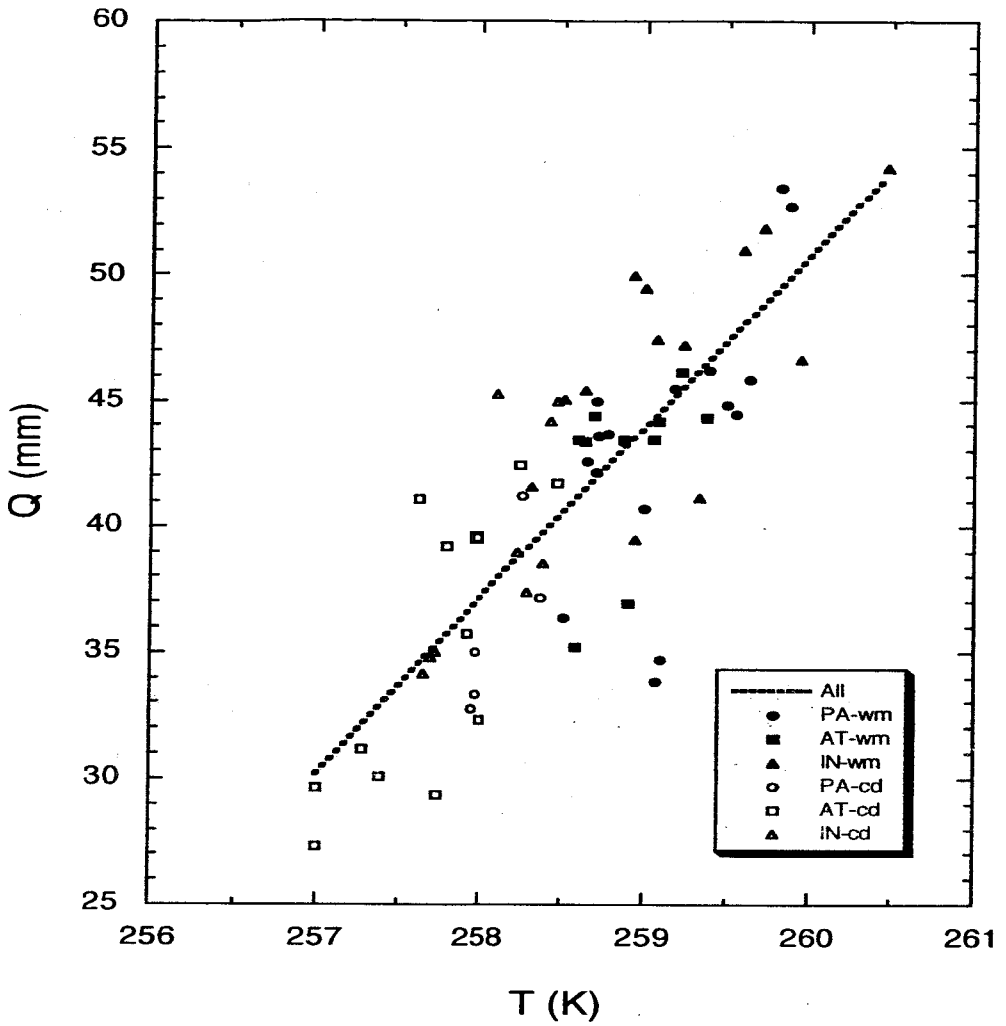

Fig. 1. Scatter diagram of domain-averaged water vapor versus temperature for three oceanic regions - "Atlantic" (22^0S-22^0N, 65^0W-15^0W), "Indian" (22^0S-10^0N, 40^0E-110^0E) and "Pacific" Ocean (22^0S-22^0N, 120^0E-120^0W), respectively, in "warm" (denoted as "wm") and "cold"(denoted as "cd") months. The relatively warm and cold regimes are divided based on a criterion temperature of 258.5 (K) (see details in Table 1). A regression line (thick dotted line) with a slope of 6.8 (mm K^{-1}) obtained by applying a linear regression method to the group including all data points is also shown.

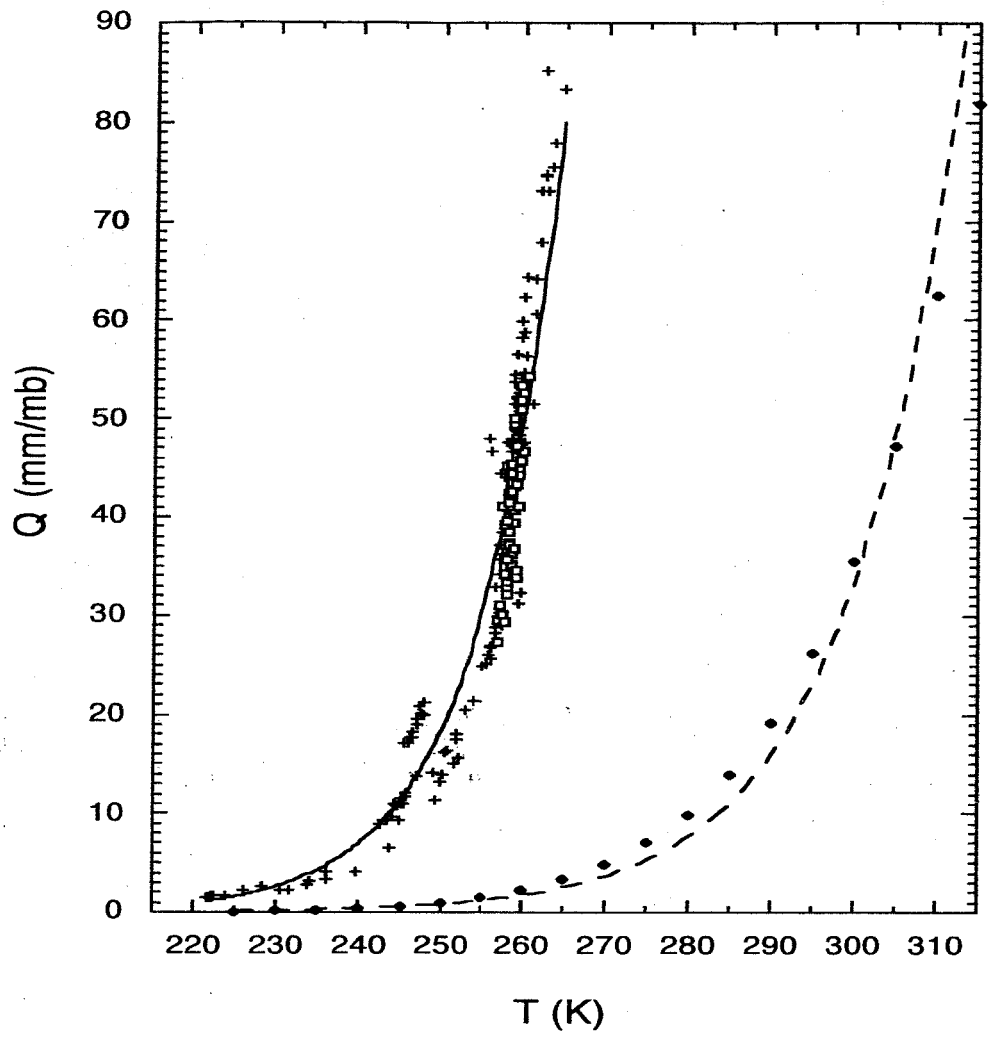

Fig. 2. The oceanic domain-averaged water vapor (mm)-temperature (K) (also shown in Fig. 1) (open squares), along with the curvilinear distribution of domain-averaged water vapor-temperature for 135 data points from global regions (crosses and solid curve) and the curvilinear distribution of saturated water vapor pressure (mb)-temperature obtained based on the Clausius-Clapeyron equation (dark diamonds and dashed curve) (adopted from Fig. 4 in Shie et al. 2005). The curvilinear lines are obtained using an exponential fitting.

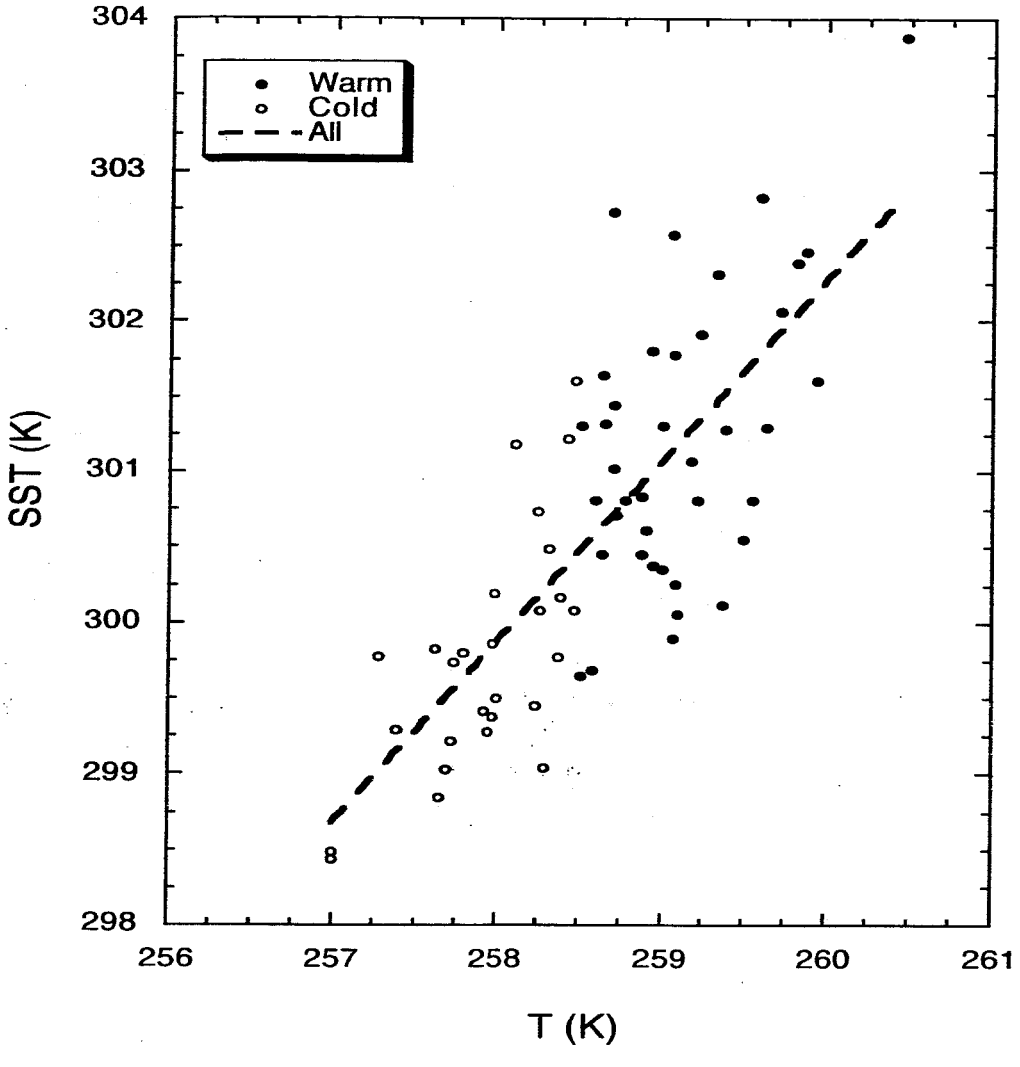

Figure 3. Scatter diagram of domain-averaged SST versus temperature for the six "seasonal" ocean groups (same as those in Fig. 1) with the open and dark circles denoting data from the "Cold" and "Warm" months, respectively. A regression line (thick dashed line) with a slope of 1.2 ($K K^{-1}$) obtained by applying a linear regression method to the group including all data points is also shown.

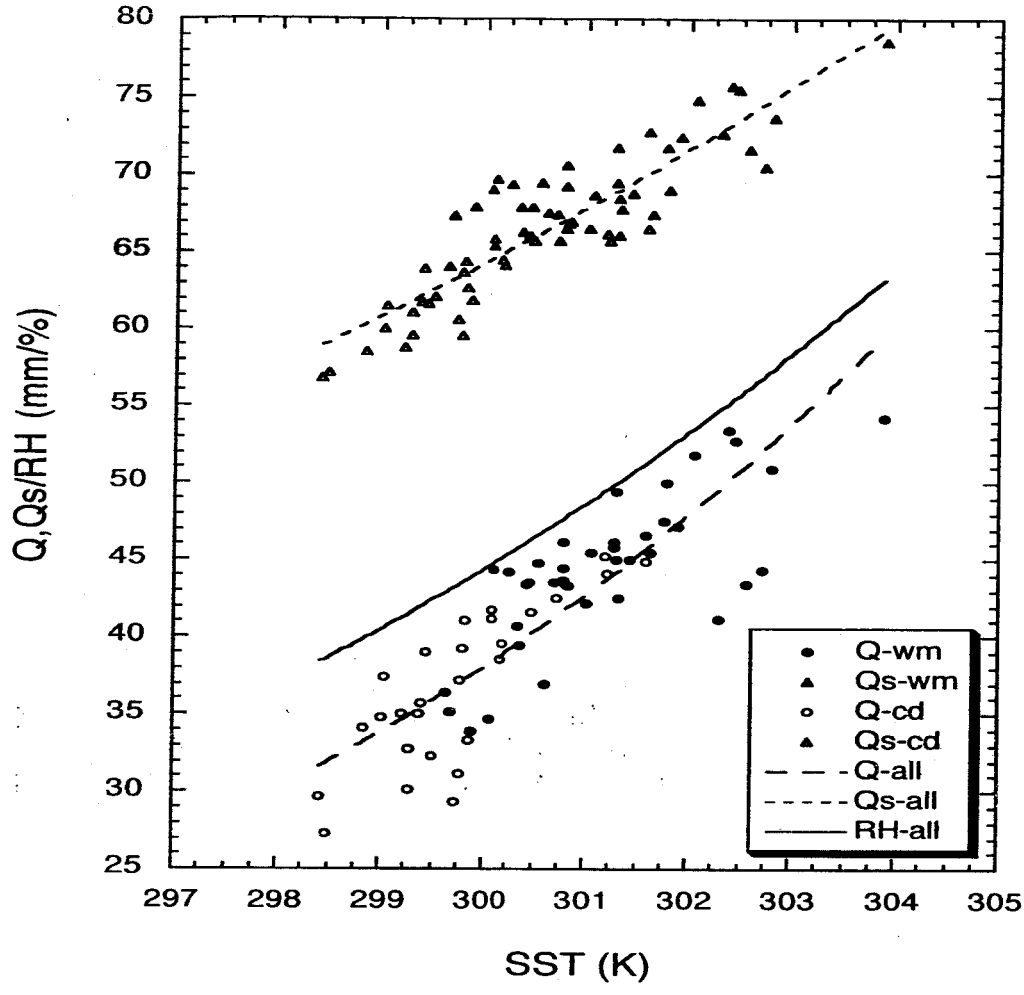

Fig. 4. The distribution of domain-averaged water vapor and saturated water vapor (mm) versus SST (K) for the six "seasonal" ocean groups (same as those in Fig. 1) with the dark and open circles/triangles denoting water vapor/saturated water vapor from the warm and cold months, respectively. The respective curvilinear lines are obtained including all the water vapor (thick dashed line) and saturated water vapor (thick dotted line) data points using an exponential regression fitting. A regression line obtained by including all the relative humidity (%) data points is also shown (thick solid line). The individual relative humidity data points are not shown here for the sake of figure clarity.

A Note on the Relationship between Temperature and Water Vapor over Oceans, including Sea Surface Temperature Effect

C.-L. Shie, W.-K. Tao and J. Simpson

Popular Summary

This note follows up on a recent study by Shie et al. (2005) and extends the investigation of the domain-averaged moisture-temperature (Q-T) relationship from the Tropics (i.e., the previous study) to the tropical Pacific, Atlantic and Indian Oceans. The Q and T data examined in this study are obtained from the GEOS-3 [Goddard Earth Observing System Version-3] global re-analysis monthly products. Similar to what was found earlier in the Tropics, Q is also found to increase with T over the entire oceanic region; however, Q increases faster with T over oceans than over the Tropics. The Q-T distribution for the Tropics is in a quasi-linear relationship, which is embedded in a global Q-T distribution that is, however, in a more complex curvilinear relationship. The Q-T distribution over the oceanic regions seems to fall within the lower bound (i.e., the relatively colder and driver regime) of the tropical Q-T distribution. T over oceans is also found increasing with SST (sea surface temperature), which seemingly implies that an air mass might have gained heat more readily from a warmer ocean as compared to a colder ocean. Q is also found to increase with SST in a manner that quantitatively resembles an earlier finding by Stevens (1990). We also found that relative humidity exhibits similar behaviors for oceanic and tropical regions, respectively, i.e., it increases with both SST and T over oceans and increases with T in the Tropics (Shie et al. 2005). All these similar features found between oceanic and tropical regions seem to inform us that oceans occupy most of the Tropics and so play a key role in determining what have happened in the Tropics.